Gu et al. Molecular Brain (2015) 8:15
DOI 10.1186/s13041-015-0105-2

Molecular Brain

RESEARCH Open Access

Dexmedetomidine inhibits Tetrodotoxin-resistant $Na_v1.8$ sodium channel activity through $G_{i/o}$-dependent pathway in rat dorsal root ganglion neurons

Xi-Yao Gu[1†], Ben-Long Liu[1†], Kai-Kai Zang[1], Liu Yang[1], Hua Xu[2], Hai-Li Pan[3], Zhi-Qi Zhao[1] and Yu-Qiu Zhang[1*]

Abstract

Background: Systemically administered dexmedetomidine (DEX), a selective α2 adrenergic receptor (α2-AR) agonists, produces analgesia and sedation. Peripherally restricted α2-AR antagonist could block the analgesic effect of systemic DEX on neuropathic pain, with no effect on sedation, indicating peripheral analgesic effect of DEX. Tetrodotoxin-resistant (TTX-R) sodium channel $Na_v1.8$ play important roles in the conduction of nociceptive sensation. Both α2-AR and Nav1.8 are found in small nociceptive DRG neurons. We, therefore, investigated the effects of DEX on the $Na_v1.8$ currents in acutely dissociated small-diameter DRG neurons.

Results: Whole-cell patch-clamp recordings demonstrated that DEX concentration-dependently suppressed TTX-R $Na_v1.8$ currents in small-diameter lumbar DRG neurons. DEX also shifted the steady-state inactivation curves of $Na_v1.8$ in a hyperpolarizing direction and increased the threshold of action potential and decrease electrical and chemical stimuli-evoked firings in small-diameter DRG neurons. The α2-AR antagonist yohimbine or $\alpha2_A$-AR antagonist BRL44408 but not $\alpha2_B$-AR antagonist imiloxan blocked the inhibition of $Na_v1.8$ currents by DEX. Immunohistochemistry results showed that $Na_v1.8$ was predominantly expressed in peripherin-positive small-diameter DRG neurons, and some of them were $\alpha2_A$-AR-positive ones. Our electrophysiological recordings also demonstrated that DEX-induced inhibition of $Na_v1.8$ currents was prevented by intracellular application of G-protein inhibitor GDPβ-s or $G_{i/o}$ proteins inhibitor pertussis toxin (PTX), and bath application of adenylate cyclase (AC) activator forskolin or membrane-permeable cAMP analogue 8-Bromo-cAMP (8-Br-cAMP). PKA inhibitor Rp-cAMP could mimic DEX-induced inhibition of $Na_v1.8$ currents.

Conclusions: We established a functional link between α2-AR and $Na_v1.8$ in primary sensory neurons utilizing the $G_{i/o}$/AC/cAMP/PKA pathway, which probably mediating peripheral analgesia of DEX.

Keywords: α2-adrenoceptor, Dexmedetomidine, Dorsal root ganglion, Pain, Tetrodotoxin-resistant (TTX-R) sodium channel $Na_v1.8$, Whole-cell recording

* Correspondence: yuqiuzhang@fudan.edu.cn
†Equal contributors
[1]Institute of Neurobiology, Institutes of Brain Science and State Key Laboratory of Medical Neurobiology, Collaborative Innovation Center for Brain Science, Fudan University, 138 Yi Xue Yuan Road, Shanghai 200032, China
Full list of author information is available at the end of the article

Background

Dexmedetomidine (DEX), a potent and highly selective agonist of the alpha 2 adrenergic receptors (α2-ARs) with more favorable pharmacokinetic properties than clonidine (another commonly used α2-AR agonist) is approved for the adult intensive care unit use as sedative infusion by the US Food and Drug Administration in 1999. Three α2-ARs ($\alpha2_A$-, $\alpha2_B$- and $\alpha2_C$-ARs) have been cloned, and all of which are coupled to inhibitory G proteins [1] and play an important role in the control of pain. The α2-ARs have a diffuse distribution in the nervous system, including in primary afferents, spinal dorsal horn and brain stem [2-5]. Systemically administered α2-AR agonists produce anti-nociceptive effects in humans and animals, suggesting that the α2-AR may be involved in anti-nociception at the supraspinal, spinal and peripheral levels [6-9]. Our previous study showed that intrathecal DEX significantly suppressed monoarthritis-induced thermal hyperalgesia and glial activation in spinal level [10]. However, intrathecal or intracerebroventricular administration of DEX produces dose-dependent sedation [11]. Peripherally restricted α2-AR antagonist could block the analgesic effect of systemic DEX on neuropathic pain, with no effect on sedation, indicating peripheral analgesic effect of DEX [7].

Evidence has emerged that the effects on ion channels may be an important mechanism underlying DEX-induced peripheral anti-nociception [12,13]. Previous studies have revealed that changes in function of voltage-gate sodium channels in nociceptive primary sensory neurons participate in the development of peripheral hyperexcitability that occurs in neuropathic and inflammatory pain conditions [14,15]. Among them, the tetrodotoxin-resistant (TTX-R) sodium channel $Na_v1.8$ primarily expressed by small- and medium-sized dorsal root ganglion (DRG) neurons [16,17], substantially contributes to the upstroke of action potential in these neurons [18]. $Na_v1.8$-null mice displayed a pronounced increase in threshold to noxious mechanical stimuli and a slight decrease in nociceptive thermoreception as well as delayed development of inflammatory hyperalgesia [19]. Likewise, functional knockdown of $Na_v1.8$ in rats reduces hyperalgesia and allodynia in neuropathic pain and inflammatory pain models [14,20,21]. Several G-protein-coupled receptors (GPCRs)-mediated second-messenger cascades including PKA, PKC and MAPKs have been shown to regulate $Na_v1.8$ sodium channels [14,22]. In the present study, we investigated whether the peripheral DEX-induced analgesia might in part arise from the suppressed activation of TTX-R sodium channel $Na_v1.8$ currents via binding to its GPCR α2-ARs in small-diameter DRG neurons.

Results

Recording of Nav1.8 currents in DRG neurons

Double immunofluorescence revealed that $Na_v1.8$ was predominantly expressed in peripherin-positive small-diameter DRG neurons (Figure 1A). In the present study, all recordings were performed in small-diameter (<25 μm) DRG neurons. With existence of TTX (500 nM) in external solution, TTX-resistant (TTX-R) sodium currents were recorded in most (170 out of 223) of the small-diameter DRG neurons. As our previous reported, the membrane potential was held at −60 mV to inhibit $Na_v1.9$ currents, leaving the $Na_v1.8$ currents intact [22]. The family of $Na_v1.8$ currents was generated with a voltage-clamp protocol (holding at -60 mV, depolarizing steps from -55 mV to +40 mV, 50 ms, 5 mV increment, Figure 1B). According to the current–voltage relationship (Figure 1C), we selected -15 mV to elicit $Na_v1.8$ currents in most of the recordings (Figure 1D). The peak amplitude of $Na_v1.8$ currents was stable during the recordings.

Effects of DEX on $Na_v1.8$ currents in small DRG neurons

Application of DEX in different doses (0.03, 0.1, 0.3, 1, 3 and 30 μM) dose-dependently reduced the peak amplitude of $Na_v1.8$ currents in small DRG neurons within 1 min and washed out within 5 min (Figure 2A and B). One-way ANOVA analysis revealed a significant effect of DEX treatment ($F_{6,66} = 23.885$, $p < 0.001$). The ED_{50} was calculated to be 0.92 μM (95% CI: 0.77–1.68). The maximal inhibitory effect (36.51 ± 5.39%) was induced by 3 μM DEX. A higher concentration of DEX (30 μM) failed to induce more powerful inhibition (34.56 ± 2.7%), indicating a "ceiling effect" at a concentration of 3 μM (Figure 2C).

The effects of DEX on the activation and inactivation properties of $Na_v1.8$ currents were studied using the appropriate voltage protocols. As described above, a voltage-clamp protocol consisted of 50 ms depolarizing steps from -55 mV to +40 mV with 5 mV increment was used to determine the activation of $Na_v1.8$ channels. No shift in the voltage-dependent activation curve was observed in DEX-treated group compared with control one (Figure 3A). The half-maximal activation potential ($V_{1/2\ activation}$) was −27.30 ± 2.13 mV (n = 7) and −28.17 mV ± 0.73 mV (n = 7) in the absence and presence of 3 μM DEX, respectively. Steady-state inactivation of $Na_v1.8$ channel was determined at a series of membrane potentials from −60 mV to −20 mV with 5 mV increment for 500 ms and a following test potential of −15 mV. DEX caused a left shift toward the hyperpolarizing potential of the steady-state inactivation curve (Figure 3B). The $V_{1/2\ inactivation}$ was −40.49 ± 2.49 mV (n = 9) of the control and −45.39 ± 2.65 mV (n = 9) of DEX treatment, respectively.

DEX reduced $Na_v1.8$ currents via $\alpha2_A$-AR

DEX was a selective alpha 2 adrenergic receptor (α2-AR) agonist. To address whether the attenuation of $Na_v1.8$ currents induced by DEX application was mediated by α2-ARs, the effect of yohimbine, an α2-ARs antagonist, on inhibitory effects of DEX on $Na_v1.8$ currents was

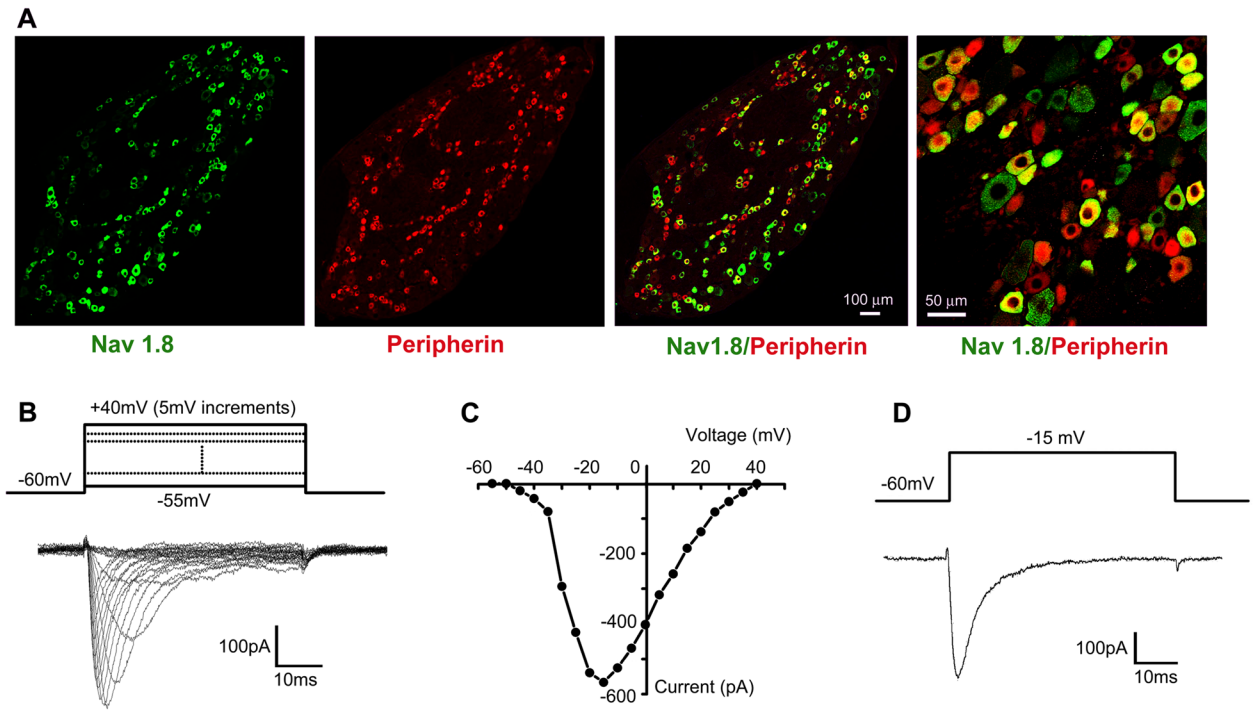

Figure 1 Isolation of TTX-resistant $Na_v1.8$ currents in small-diameter DRG neurons. (A) Double immunofluorescence reveals the expression of $Na_v1.8$ in peripherin-positive small-diameter DRG neurons. **(B)** Representative *I-V* curve family of currents recorded in the presence of 500 nM TTX. Cells were depolarized to a variety of potentials (−55 mV to +40 mV) from a holding potential of -60 mV, to elicit $Na_v1.8$ currents. **(C)** *I-V* curve of $Na_v1.8$ currents shown in (B). **(D)** Representative traces of $Na_v1.8$ currents elicited by a single pulse of −15 mV.

examined. Like previous report [12], yohimbine (30 μM) per se inhibited $Na_v1.8$ currents (Figure 4A). Pretreatment of DRG neurons with 3 μM yohimbine, a concentration to antagonize DEX-induced membrane hyperpolarization mediated by α2-ARs in rat hypothalamic neurons [23], DEX-induced suppression of the $Na_v1.8$ currents was significantly blocked (Figure 4B and C). The peak densities of $Na_v1.8$ currents in yohimbine (3 μM) plus DEX (3 μM)-treated group was significantly greater than that in DEX-treated group (One-way ANOVA, $F_{3,\ 26} = 5.451$, $p < 0.01$). Moreover, we examined the effect of BRL44408 (a preferential $\alpha2_A$-AR antagonist) on DEX-induced inhibition of $Na_v1.8$ currents. Pre-incubation of BRL44408 (1 μM) alone did not affect the peak densities of $Na_v1.8$ currents, but significantly blocked DEX-induced suppression of $Na_v1.8$ currents (Figure 4D and F). Given that BRL44408 may also be able to block $\alpha2_B$-AR at a higher dose, we further examined the effect of $\alpha2_B$-AR antagonist imiloxan on DEX-induced inhibition of $Na_v1.8$ currents. Neither basal $Na_v1.8$ currents nor DEX-induced suppression was influenced by incubation of imiloxan (3 μM) (Figure 4E and F). These data indicated that DEX

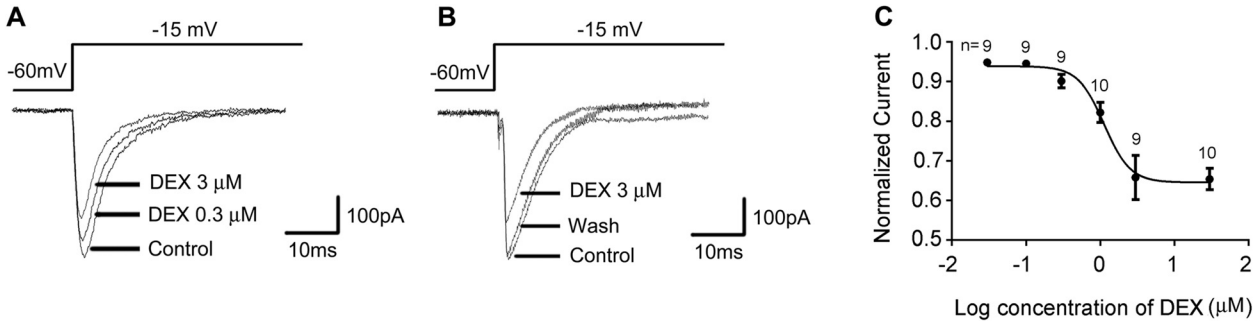

Figure 2 DEX dose-dependently inhibits $Na_v1.8$ currents. (A, B) Typical traces illustrating the $Na_v1.8$ currents in small-diameter DRG neurons recorded pre- (control) and post- (DEX) perfusion of DEX and wash out. **(C)** Dose-effect curve of DEX-induced inhibition of $Na_v1.8$ currents. The currents were measured after a 1-min application of different concentrations of DEX.

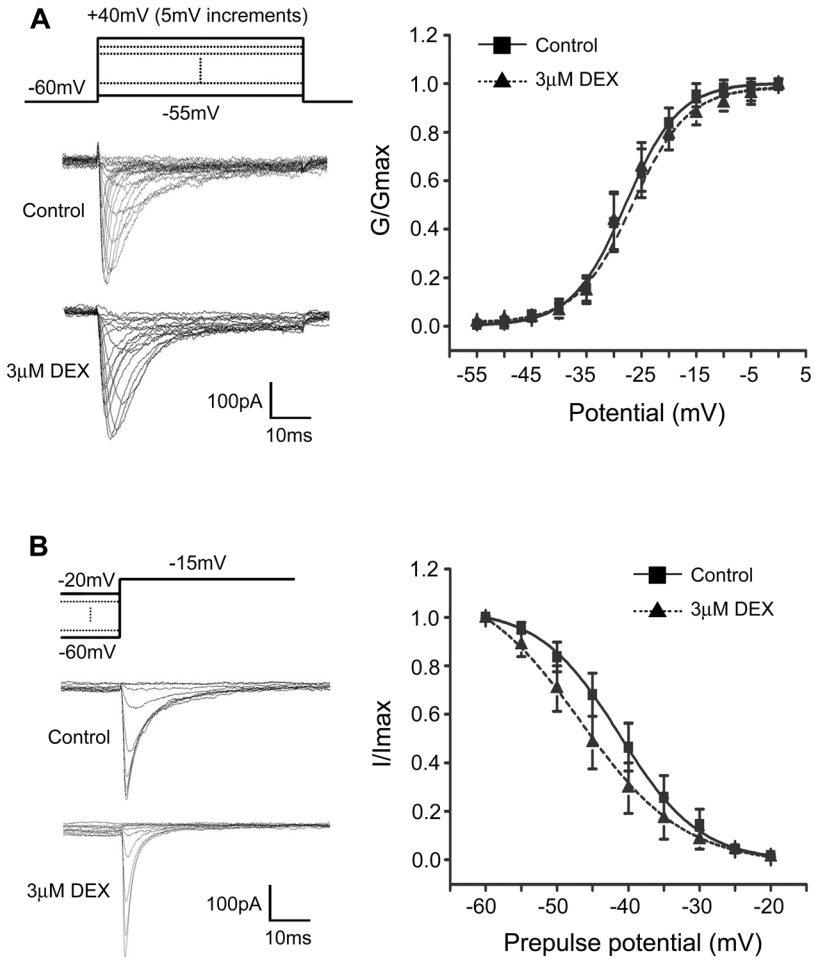

Figure 3 Effect of DEX on the steady-state activation and inactivation curves of $Na_v1.8$. (A) DEX (3 μM) did not shift voltage-dependent activation curve. **(B)** DEX (3 μM) shifted the steady-state inactivation curve in a hyperpolarizing direction.

modulated $Na_v1.8$ currents mainly through $\alpha2_A$-AR. Also, the colocalization of $Na_v1.8$ with $\alpha2_A$-AR in DRG small-diameter neurons provided a cellular basis for the involvement of $\alpha2_A$-AR in the DEX modulating $Na_v1.8$ currents (Figure 4G).

$G_{i/o}$-proteins participate in DEX-induced $Na_v1.8$ currents inhibition

Given α2-ARs act through G-proteins, we examined the effect of GDPβ-s, a G protein inhibitor, on DEX-induced rapid suppression of $Na_v1.8$ currents in small DRG neurons. Inclusion in pipette solution of GDPβ-s (1 mM) did not impair $Na_v1.8$ activation. On the other hand, the inhibition of $Na_v1.8$ currents by DEX was completely abolished (Figure 5A and C) (One-way ANOVA, $F_{3,38} = 12.757$, $p < 0.01$).

$\alpha2_A$-ARs are generally known to coupled to the inhibitory G_i proteins [24] through which they inhibit adenylate cyclase (AC) activity. Therefore, we examined whether DEX-induced inhibition of $Na_v1.8$ currents occurs via Gi proteins. As shown in Figures 5B and C, pertussis toxin (PTX, 1 μg/ml), an irreversible inhibitor of $G_{i/o}$-proteins, significantly prevented the $Na_v1.8$ currents amplitude change induced by DEX (One-way ANOVA, $F_{3,30} = 15.765$, $p < 0.01$). Inclusion in pipette solution of PTX (1 μg/ml) did not change $Na_v1.8$ currents amplitude (Figure 5B and C).

Because G_i proteins inhibit the catalytic activity of AC, which catalyzes cAMP production, the G_i-mediated suppression of $Na_v1.8$ currents can be the consequence of decreased levels of intracellular cAMP and a concomitant reduction in PKA-dependent phosphorylation of $Na_v1.8$. Here, we used Rp-cAMP, 8-Br-cAMP and forskolin to examine the effects of AC-cAMP-PKA pathway on the $Na_v1.8$ currents. Incubate with PKA inhibitor Rp-cAMP (50 μM) for 5 min, $Na_v1.8$ currents were significantly suppressed. Co-application of 3 μM DEX did not cause a further reduction of the currents amplitudes (Figure 5D and E). Moreover, 5-min pretreatment of DRG neurons with 8-Br-cAMP (500 μM) a membrane-permeable cAMP

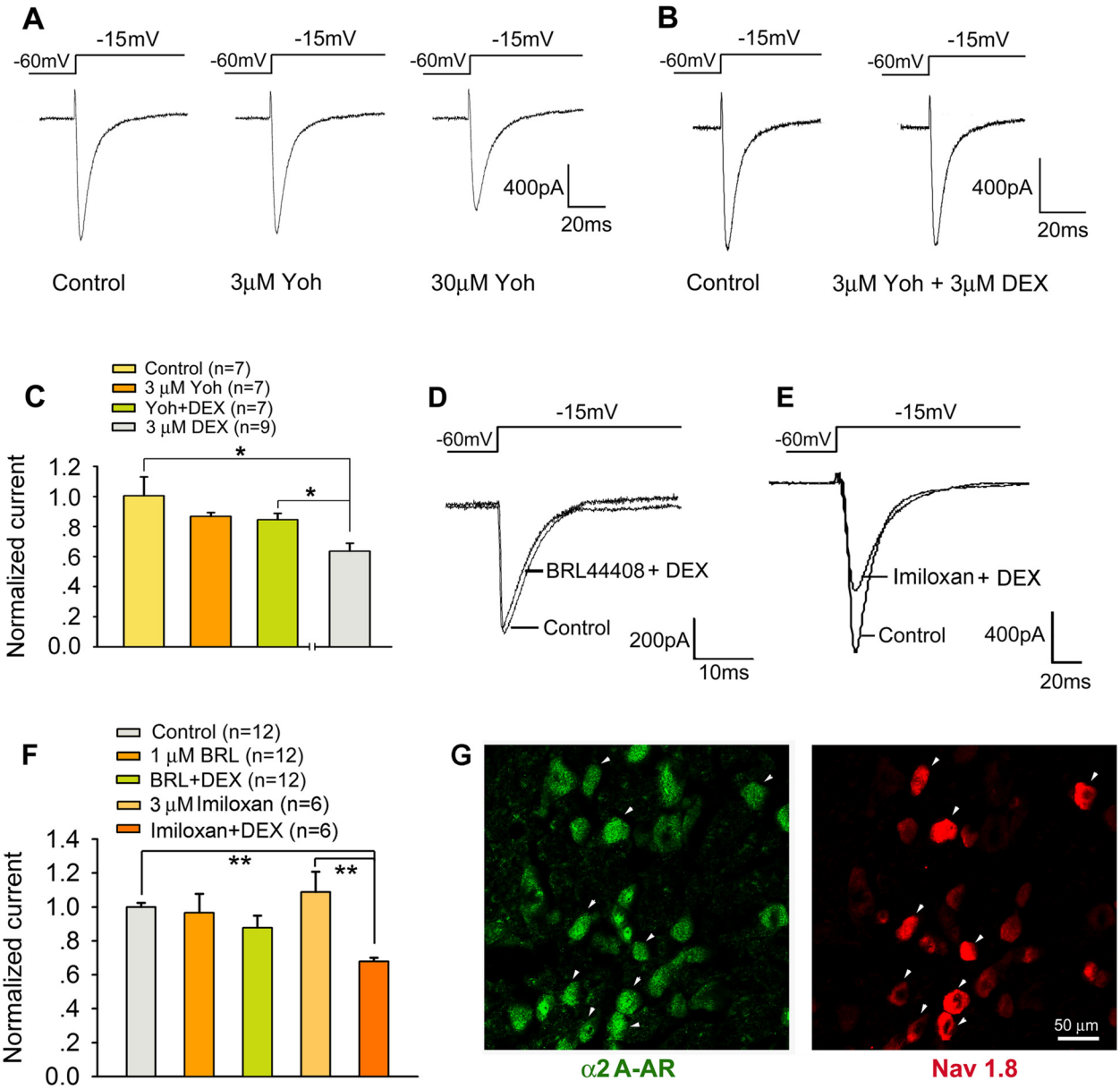

Figure 4 α2-AR mediates inhibition of DEX on $Na_v1.8$ currents. (A) The effects of different doses of yohimbine (α2-AR antagonist) on $Na_v1.8$ currents. **(B, C)** pre-incubation of yohimbine (3 μM) for 30 min blocked the inhibitory effect of DEX (3 μM) on $Na_v1.8$ currents. *$p < 0.05$. **(D-F)** DEX-induced inhibition of $Na_v1.8$ currents were completely blocked by pre-incubation of $\alpha2_A$-AR antagonist BRL44408 (1 μM) but not by $\alpha2_B$-AR antagonist imiloxan (3 μM). **(G)** Immunofluorescence micrographs of two adjacent sections from a DRG (L5) after incubation with $\alpha2_A$-AR antibody and $Na_v1.8$ antibody. Arrowhead indicates coexistence between $\alpha2_A$-AR and $Na_v1.8$ in the same neurons.

analogues, or forskolin (0.1 μM), a AC activator, caused slight increase in $Na_v1.8$ currents amplitude (Figure 5 F-I). Although the increase did not reach statistical significance, it totally removed the inhibitory effect of DEX on $Na_v1.8$ currents (Figure 5G and I).

Effect of dexmedetomidine on excitability of DRG neurons

$Na_v1.8$ is the main contributor to the upstroke of action potentials in small-diameter DRG neurons [18]. Thus, modulation of this channel by DEX should influence the excitability of DRG neurons. We applied 10 ms step depolarizing currents pulse to evoke action potentials. In 13 of 23 neurons tested, DEX 3 μM significantly increase the injected currents threshold to evoke action potentials from 37.5 ± 4.97 pA to 61.88 ± 5.78 pA before and after exposure to DEX respectively (paired *t*-test, $p < 0.01$) (Figure 6A and B). Moreover, by injection of maximum currents pulse (500 ms, 200 pA), action potential firing

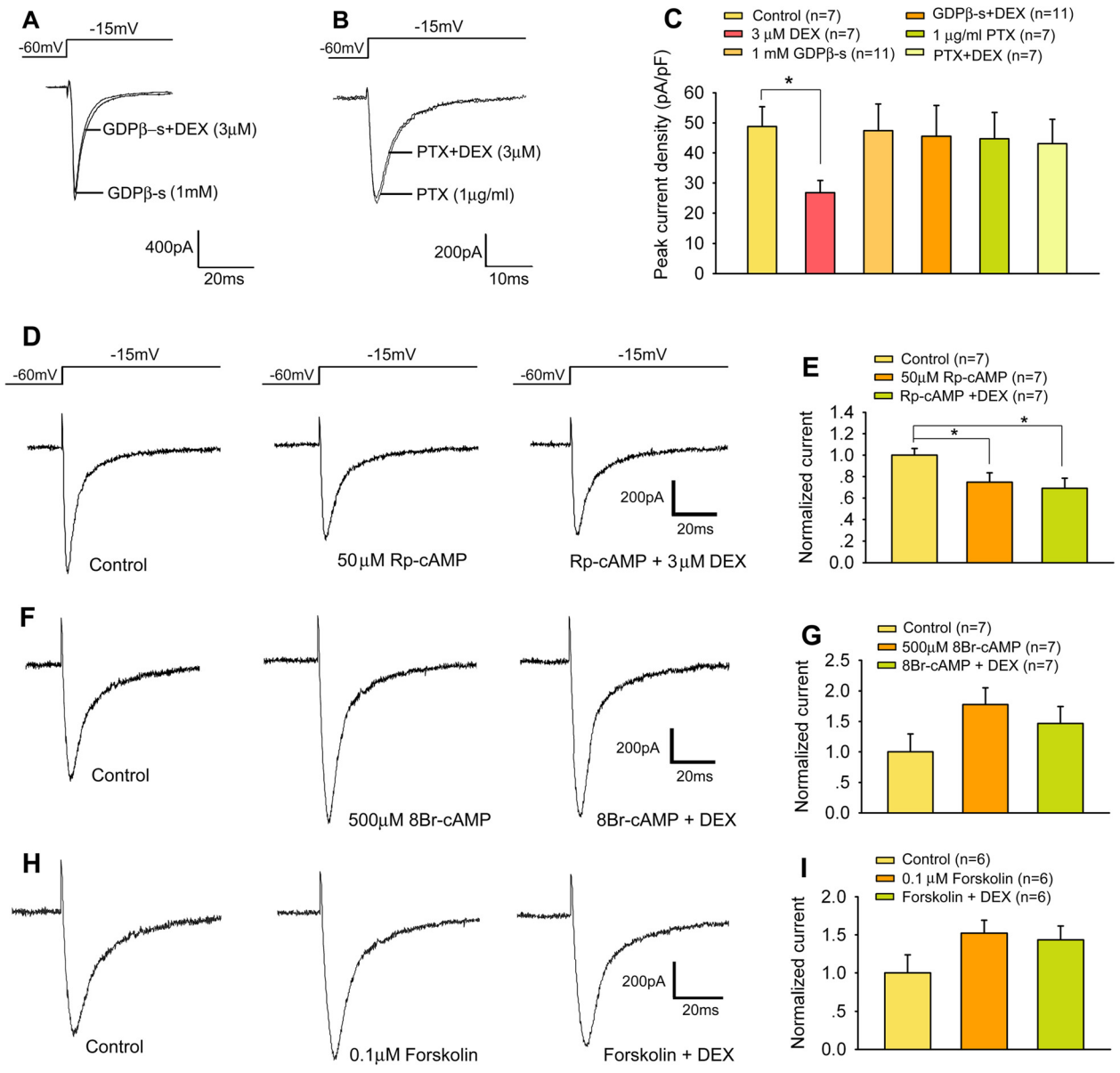

Figure 5 Involvement of $G_{i/o}$ proteins/AC/cAMP/PKA pathway in DEX-induced inhibition of $Na_v1.8$ currents. (A-C) Loading neurons with 1 mM GDPβ-s or PTX completely abolished the inhibitory effect of DEX on $Na_v1.8$ currents. *p < 0.05. **(D, E)** Pre-incubation PKA inhibitor Rp-cAMP (50 μM) inhibited $Na_v1.8$ currents. Co-application of DEX did not cause a further reduction of the current amplitudes. *p < 0.05. **(F, G)** Pre-incubation cAMP analogues 8-Br-cAMP (500 μM) prevented DEX-induced inhibition of $Na_v1.8$ currents. **(H, I)** Pre-incubation AC activator forskolin (0.1 μM) prevented DEX-induced inhibition of $Na_v1.8$ currents.

frequencies of DRG neurons were significantly decreased by DEX treatment (Figure 6C and E). DEX-induced inhibitory effect on action potential firing can be mimicked by selective $\alpha2_A$-AR agonist guanfacine (30 μM) (Figure 6D and E). Similarly, 0.5 μM capsaicin-induced action potentials were also significantly blocked by DEX (Figure 6F and G).

Discussion

In this study, we demonstrated that selective α2-AR agonist dexmedetomidine (DEX) reduced $Na_v1.8$ currents in small-diameter acutely dissociated DRG neurons. We also showed that DEX decreased excitability of small sensory neurons by increasing the activation threshold and decreasing the action potential firing. This inhibition of $Na_v1.8$ currents was completely blocked by the selective $\alpha2_A$-AR antagonist, suggesting that $\alpha2_A$-AR might be directly involved in DEX-induced changes in $Na_v1.8$ activity. We also found that the PTX-sensitive $G_{i/o}$ proteins/AC/cAMP/PKA signaling cascade is primarily responsible for the activation of $Na_v1.8$ currents in response to DEX

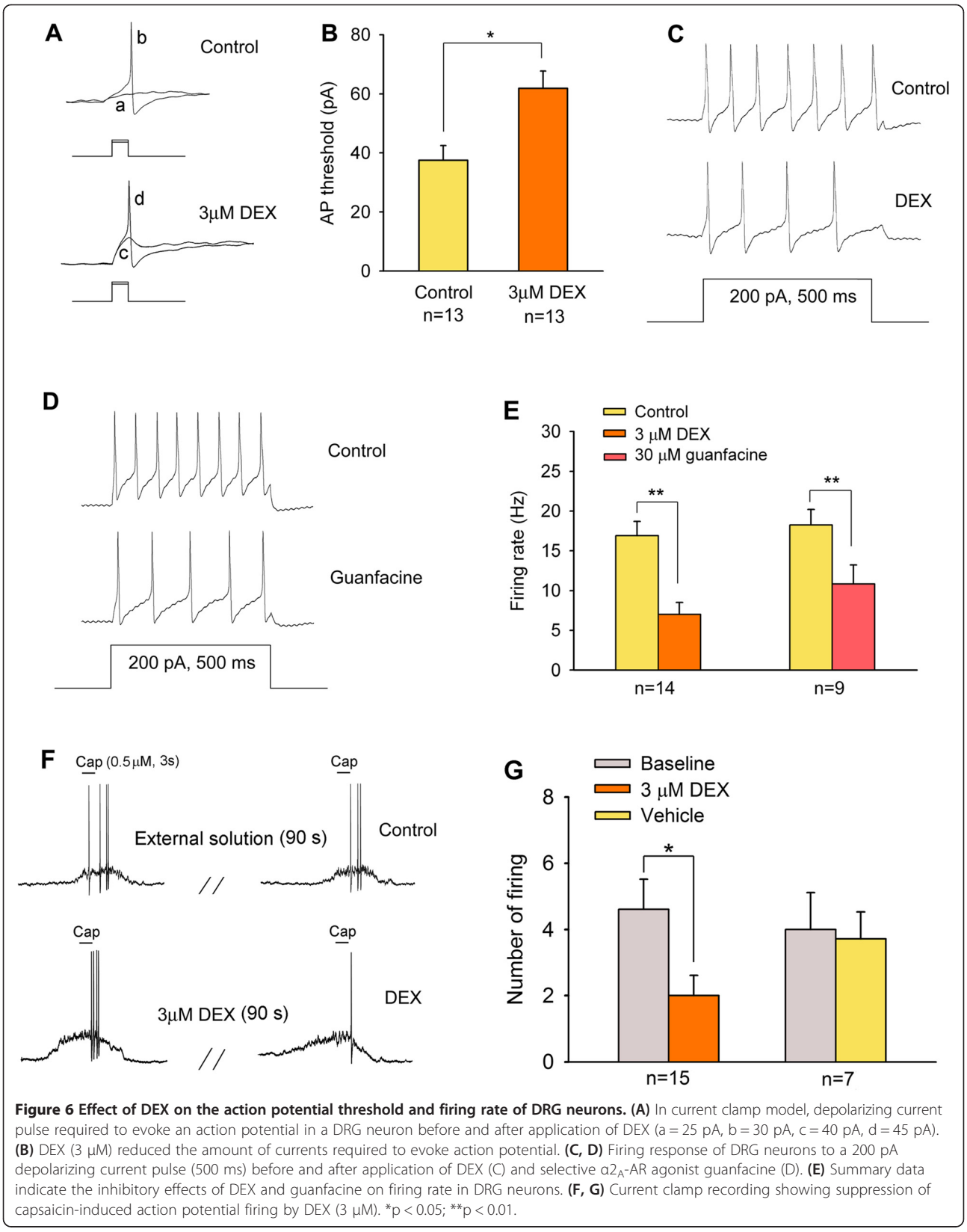

Figure 6 Effect of DEX on the action potential threshold and firing rate of DRG neurons. (A) In current clamp model, depolarizing current pulse required to evoke an action potential in a DRG neuron before and after application of DEX (a = 25 pA, b = 30 pA, c = 40 pA, d = 45 pA). **(B)** DEX (3 μM) reduced the amount of currents required to evoke action potential. **(C, D)** Firing response of DRG neurons to a 200 pA depolarizing current pulse (500 ms) before and after application of DEX (C) and selective $\alpha 2_A$-AR agonist guanfacine (D). **(E)** Summary data indicate the inhibitory effects of DEX and guanfacine on firing rate in DRG neurons. **(F, G)** Current clamp recording showing suppression of capsaicin-induced action potential firing by DEX (3 μM). *p < 0.05; **p < 0.01.

in DRG neurons. These results suggest a peripheral mechanism of DEX analgesia.

TTX-R sodium channel primarily expresses in DRG nociceptors [25,26]. In the two distinct TTX-R sodium channel isoforms $Na_v1.8$ and $Na_v1.9$, $Na_v1.8$ likely mediates the majority of TTX-R currents. Accumulating evidence points up that TTX-R sodium channel plays an important role in peripheral pain processing [27]. Nociceptive signals evoke a dynamic change of TTX-R sodium channel, for example, chronic compression (CCD) of the DRG [15,28] or local inflammation of the DRG by the application of zymosan [29] and subcutaneous injection of carrageenan [30] or complete Freund's adjuvant (CFA) [31] produces an increase in TTX-R sodium currents in small DRG neurons. Either the physiological or pathological pain was alleviated in the $Na_v1.8$-null mice or $Na_v1.8$ knockdown rats [14,27,32,33]. Peripheral inflammation or nerve injury has been shown to upregulate $Na_v1.8$ expression in nociceptive DRG neurons [34,35]. Blockade of $Na_v1.8$ sodium channel by A-803467, a potent and selective $Na_v1.8$ sodium channel blocker, could inhibit nerve injury-induced mechanical allodynia and inflammation-induced thermal hyperalgesia [36].

Given that both α2-AR and Nav1.8 are found in small nociceptive DRG neurons [4,5,37], and $\alpha2_A$-AR and $Na_v1.8$ co-localized in the same small DRG neurons, we propose that stimulation of α2-AR in sensory neurons may lead to an attenuation of the painful symptoms of hypersensitivity via the inhibition of $Na_v1.8$ channel activity. Consistently, application of DEX concentration-dependently decreased the current density of $Na_v1.8$ in small DRG neurons and shifted the voltage-dependence of steady-state inactivation curve for $Na_v1.8$ in the hyperpolarizing direction, which could result in a lower threshold for Na^+ channel inactivation. DEX also increased the threshold of action potential and decreased firing rate in small DRG neurons. Despite of the previous reports that yohimbine did not alter DEX-induced inhibition of TTX-R Na^+ currents in small DRG neurons [12] and voltage-gated Na^+ currents in NG108-15 cells [13], the present study showed that 3 μM yohimbine, a concentration to antagonize DEX-induced membrane hyperpolarization mediated by α2-ARs in rat hypothalamic neurons [23], completed blocked DEX-induced suppression of the $Na_v1.8$ currents, suggesting an involvement of α2-ARs in DEX effect. Considering the affinity of yohimbine for α1-ARs, serotonin and dopamine receptors [38], inhibition of high dose yohimbine per se on $Na_v1.8$ currents may relate to the interaction of yohimbine with these receptors.

Although three subtypes of the α2-ARs mRNAs were expressed in the rat DRGs [5,39,40], $\alpha2_B$-AR mRNA was only found in small numbers of neuron profiles [5,41], and following peripheral nerve injury, $\alpha2_A$-AR and $\alpha2_C$-AR mRNA levels increased and decreased, respectively [5,40]. Also, the immunohistochemical analysis showed that $\alpha2_A$-AR and $\alpha2_C$-AR proteins in DRG neurons was respectively increased and decreased after chronic constriction injury of sciatic nerve, whereas no $\alpha2_B$-AR neurons were detected in either normal or nerve injury DRG [42]. Moreover, $\alpha2_A$-AR rather than $\alpha2_C$-AR in the superficial layers of spinal dorsal horn was observed in the terminals of capsaicin-sensitive and substance P-containing primary afferent fibers [2]. Degeneration of TRPV1 afferent terminals, the level of $\alpha2_A$-AR, but not $\alpha2_C$-AR, was largely reduced in primary afferent terminals [43]. Our present study further showed co-localization of $\alpha2_A$-AR- and $Na_v1.8$-like immunoreactivity in small DRG neurons. DEX-induced inhibition of $Na_v1.8$ currents was prevented by pretreatment of BRL44408, a preferential $\alpha2_A$-AR antagonist, but not of imiloxan, a $\alpha2_B$-AR antagonist. In addition to $Na_v1.8$, other cation channels, for example, TRPM8 may also participate in $\alpha2_A$-AR-mediated nociceptive inhibition. Stimulation of $\alpha2_A$-AR inhibited TRPM8 in DRG neurons [44]. Taken together, these findings suggest that the $\alpha2_A$-AR subtype represents the most likely candidate in DRG neurons to be involved in the modulation of nociceptive information.

Our data strongly suggest that DEX inhibits $Na_v1.8$ currents in a $G_{i/o}$ proteins/AC/cAMP/PKA signaling-dependent manner in small DRG neurons. Specifically, we showed that preventing $G_{i/o}$ recruitment by PTX treatment blocked DEX-induced inhibition of $Na_v1.8$ current density, and PKA inhibitor mimicked the effect of DEX through the receptor. In support of this, it has been also reported that blockade of PKA activity inhibited the baseline $Na_v1.8$ currents in small-diameter nodose ganglion neurons [45]. Consistent with the general notion that stimulation of $\alpha2_A$-AR by DEX brings about G_i-mediated inhibition of AC and reduction of intracellular cAMP levels, AC activator forskolin and cAMP analogues 8Br-cAMP completely reversed DEX-induced inhibition of $Na_v1.8$ currents. These findings suggest that the classical AC/cAMP/PKA signaling pathway resulting from the α2-ARs-mediated activation of PTX-sensitive $G_{i/o}$ proteins is involved in the regulation of $Na_v1.8$ by DEX.

Conclusions

DEX attenuated TTX-R sodium channel $Na_v1.8$ currents in small-diameter DRG neurons via $\alpha2_A$-AR/$G_{i/o}$/AC/cAMP/PKA cascade, which probably constitutes a mechanism of peripheral DEX analgesia.

Materials and methods

Animals

Male adult (100–150 g) Wistar rats were obtained from the Experimental Animal Center, Shanghai Medical College of Fudan University, China. Rats were on a 12 h

light/dark cycle with a room temperature of 23 ± 1°C and received food and water *ad libitum*. All experiments protocols were permitted by the Shanghai Animal Care and Use Committee and followed the policies issued by the International Association for the Study of Pain on the use of laboratory animals. All efforts were made to minimize animal suffering and reduce the numbers of animals used.

Preparation of DRG neurons

Animals were anesthetized with ether and rapidly decapitated. DRGs from L4-L6 lumbar segments were removed and immediately transferred onto DMEM (Gibco, Life Technologies, Grand Island, NY, USA) on ice. The ganglia were minced with fine spring scissors and treated with collagenase (2.67 mg/ml, type IA, Sigma, St. Louis, MO) and trypsin (1 mg/ml, type I, Sigma) in DMEM saturated with CO_2/O_2 mixed gas at 37°C for 35 min. After wash with standard external solution (in mM, 150 NaCl, 5 KCl, 2 CaCl2, 1 MgCl2, 10 HEPES, and 10 glucose, adjusted to pH 7.4 with NaOH) three times, the ganglia were then gently triturated using fine fired-polished Pasteur pipettes. The dissociated DRG neurons were plated onto 10-mm diameter coverslips in the 3.5 cm culture dishes and incubated with standard external solution. Each culture dishes contained three or four coverslips and all the experiments were performed within 2–8 h after plating.

Patch-clamp recordings

Whole-cell voltage-clamp and current-clamp recordings of DRG neurons were performed at room temperature (RT, 23 ± 1°C) with an EPC-9 amplifier (HEKA Elektronik, Lambrecht/Pfalz, Germany). Stimulation protocols and data acquisition were controlled by the software Pulsefit 8.5 (HEKA Elektronik). All of the recordings were performed in small-diameter (15–25 μm) DRG neurons with resting membrane potentials more negative than −50 mV. Microelectrodes (N51A borosilicate glass, Sutter Instruments) with a resistance of 2–6 MΩ were pulled using a P97 puller (Sutter Instruments). The pipette solution contained (in mM): 140 CsF, 1$MgCl_2$, 1 EGTA, 2.5 Na2ATP, 10 HEPES, pH was adjusted to 7.2 with CsOH. Seals (1–10 GΩ) between the electrode and the cells were established. After the whole-cell configuration was established, the cell membrane capacitance and series resistance were compensated (>80%). Leak currents were subtracted using the online P/4 protocol. The data were sampled at 10 kHz and low-passed at 2 kHz. For $Na_v1.8$ recordings, the external solution contained (in mM): 32 NaCl, 20 TEA-Cl, 105 choline-Cl, 1 $MgCl_2$, 1 $CaCl_2$, 0.1 $CdCl_2$, 10 HEPES, 0.0005 TTX and 10 glucose, adjusted to pH 7.4 with NaOH. For current-clamp recordings, the electrode solution was changed to: 140 KCl, 1 $MgCl_2$, 0.5 $CaCl_2$, 5 EGTA, 10 HEPES, 2.5 Na2ATP, pH was adjusted to 7.2 with KOH. The external solution was changed to: 150 NaCl, 5 KCl, 2.5 $CaCl_2$, 1 $MgCl_2$, 10 HEPES, pH was adjusted to 7.4 with NaOH. DRG neurons were held at −60 mV and $Na_v1.8$ currents were evoked by depolarizing pulses to -15 mV. The activation and inactivation properties of $Na_v1.8$ currents were studied using the appropriate voltage protocols. The voltage-clamp protocol consisted of 50 ms depolarizing steps from -55 mV to +40 mV with 5 mV increment was used to determine the activation of $Na_v1.8$ channels. The Boltzmann function of the form $G_{Na} / G_{Namax} = 1 / \{1 + exp [(V_{m1/2} - V_m) / k]\}$ was used to describe the voltage dependence of activation and half activation potential was obtained. Steady-state inactivation of $Na_v1.8$ channel was determined at a series of membrane potentials from −60 mV to −20 mV with 5 mV increment for 500 ms and a following test potential of −15 mV. The steady-state inactivation curve was fitted by the Boltzmann function $I_{Na} / I_{Namax} = 1 / (1 + exp [(V - V_{m1/2}) / k])$, where I_{Namax} is the maximal peak current, V is the prepulse membrane potential.

Drugs

All the drugs were purchased from Sigma (St. Louis, MO, USA). The drugs were dissolved in normal saline as stock solutions. All of the stock solutions were stored at −20°C or −80°C until use. Working concentrations of the drugs were prepared on the day of the experiment from the stock solutions. The drug dosages were selected based on previous reports and our preliminary studies. Dexmedetomidine was applied continuously for 1 min closed to cells via ALA-VM8 perfusion system (ALA Scientific Instruments, Westbury, NY). Yohimbine and BRL44408 were applied to the chamber 30 min before and during the perfusion of dexmedetomidine (DEX). Rp-cAMP, 8-Br-cAMP and forskolin were applied to chamber 5–10 min before and during the DEX perfusion. GDPβ-s and PTX were applied in the pipette internal solution.

Immunohistochemistry

Animals were given an overdose of urethane and were then transcardially perfused with normal saline followed by 4% paraformaldehyde in 0.1 M phosphate buffer (pH 7.4, 4°C). DRGs (L4–L6 segments) were removed and postfixed in the same fixative for 2 h at 4°C and then immersed in a 10–30% gradient of sucrose in phosphate buffer for 24–48 h at 4°C for cryoprotection. DRGs were embedded in OCT compound, cut in a cryostat (Leica 1900, Leica) at 7 μm (to study $Na_v1.8$ and $\alpha 2_A$-AR coexistence) or 14 μm thickness and mounted onto gelatin coated slides. The sections were placed in a humid chamber and processed for immunohistochemistry. The sections were blocked with 10% donkey serum in 0.01 M PBS (pH 7.4) with 0.3% Triton X-100 for 1 h at RT. For $Na_v1.8$ and peripherin (a small-diameter DRG neuronal marker) double immunofluorescence, the sections were incubated

with a mixture of rabbit anti-$Na_v1.8$ (1:1000; Alomone) with mouse anti-peripherin (1:2000; Millipore) overnight at 4°C, followed by a mixture of Alex Flour 488- and Alex Flour 546-conjugated secondary antibodies (1:200; Invitrogen) for 2 h at 4°C. For detecting $Na_v1.8$ and $\alpha2_A$-AR coexistence, two adjacent sections (7 μm) was respectively incubated with rabbit anti-$Na_v1.8$ (1:1000) and rabbit anti-$\alpha2_A$-AR (1:100; Alomone) primary antibodies in PBS with 1% normal donkey serum and 0.3% Triton X-100 overnight at 4°C, followed by incubation within Alex Flour 546- and Alex Flour 488-conjugated secondary antibodies for 2 h at 4°C, respectively. All of the slides were coverslipped with 50% glycerin in 0.01 M PBS and then examined with an Olympus FV1000 confocal laser scanning microscope (Olympus). Images were acquired using FV10-ASW software. The specificities of the immunostaining were verified by observing no immunostaining after omitting the primary antibodies, which resulted in the disappearance of the immunostaining signals. The specificities of the primary antibodies were verified by a preabsorption experiment. Sections were first incubated overnight with a mixture of $Na_v1.8$ or $\alpha2_A$-AR primary antibody and the corresponding blocking peptide (5:1 blocking peptide: primary antibody), followed by incubation with a secondary antibody. The immunostaining signals were abolished after absorption.

Data analysis

The data were presented as means ± standard error of mean (SEM). Statistical comparisons were performed using Student's *t*-test, paired *t*-test and one-way ANOVA followed by *post hoc* Student-Newman-Keuls test. In all cases, $p < 0.05$ was considered statistically significant.

Competing interests

The authors declare that they have no competing interests.

Authors' contributions

G XY, L BL and P HL performed the patch clamp recording in DRG neurons. Z KK performed the immunofluorescence experiments. YL, XH and ZZQ participated in the statistical analysis. GXY and ZYQ conceived the study, designed the experiments, and wrote the paper. All of the authors read and approved the final manuscript.

Acknowledgements

This work was supported by the National Natural Science Foundation of China (31421091, 31420103903, 31271183 and 81471130, 81200854) and the National Basic Research Program of China (2013CB531900).

Author details

[1]Institute of Neurobiology, Institutes of Brain Science and State Key Laboratory of Medical Neurobiology, Collaborative Innovation Center for Brain Science, Fudan University, 138 Yi Xue Yuan Road, Shanghai 200032, China. [2]Department of Anesthesiology, Changhai Hospital, The Second Military Medical University, Shanghai 200433, China. [3]Center for Neuropsychiatric Diseases, Institute of Life Science, Nanchang University, Nanchang 330031, China.

Received: 30 November 2014 Accepted: 18 February 2015
Published online: 03 March 2015

References

1. Bylund DB, Blaxall HS, Iversen LJ, Caron MG, Lefkowitz RJ, Lomasney JW. Pharmacological characteristics of alpha 2-adrenergic receptors: comparison of pharmacologically defined subtypes with subtypes identified by molecular cloning. Mol Pharmacol. 1992;42(1):1–5.
2. Stone LS, Broberger C, Vulchanova L, Wilcox GL, Hökfelt T, Riedl MS, et al. Differential distribution of alpha2A and alpha2C adrenergic receptor immunoreactivity in the rat spinal cord. J Neurosci. 1998;18(15):5928–37.
3. Gold MS, Dastmalchi S, Levine JD. Alpha 2-adrenergic receptor subtypes in rat dorsal root and superior cervical ganglion neurons. Pain. 1997;69(1–2):179–90.
4. Medvedeva YV, Kim MS, Schnizler K, Usachev YM. Functional tetrodotoxin-resistant Na(+) channels are expressed presynaptically in rat dorsal root ganglia neurons. Neuroscience. 2009;159(2):559–69.
5. Shi TS, Winzer-Serhan U, Leslie F, Hökfelt T. Distribution and regulation of alpha(2)-adrenoceptors in rat dorsal root ganglia. Pain. 2000;84(2–3):319–30.
6. Aho M, Lehtinen AM, Erkola O, Kallio A, Korttila K. The effect of intravenously administered dexmedetomidine on perioperative hemodynamics and isoflurane requirements in patients undergoing abdominal hysterectomy. Anesthesiology. 1991;74(6):997–1002.
7. Poree LR, Guo TZ, Kingery WS, Maze M. The analgesic potency of dexmedetomidine is enhanced after nerve injury: a possible role for peripheral alpha2-adrenoceptors. Anesth Analg. 1998;87(4):941–8.
8. Kingery WS, Guo TZ, Davies MF, Limbird L, Maze M. The alpha(2A) adrenoceptor and the sympathetic postganglionic neuron contribute to the development of neuropathic heat hyperalgesia in mice. Pain. 2000;85(3):345–58.
9. Zhang WS, Xu H, Xu B, Sun S, Deng XM, Zhang YQ. Antihyperalgesic effect of systemic dexmedetomidine and gabapentin in a rat model of monoarthritis. Brain Res. 2009;1264:57–66.
10. Xu B, Zhang WS, Yang JL, Lû N, Deng XM, Xu H, et al. Evidence for suppression of spinal glial activation by dexmedetomidine in a rat model of monoarthritis. Clin Exp Pharmacol Physiol. 2010;37(10):e158–66.
11. Buerkle H, Yaksh TL. Pharmacological evidence for different alpha 2-adrenergic receptor sites mediating analgesia and sedation in the rat. Br J Anaesth. 1998;81(2):208–15.
12. Oda A, Iida H, Tanahashi S, Osawa Y, Yamaguchi S, Dohi S. Effects of alpha2-adrenoceptor agonists on tetrodotoxin-resistant Na + channels in rat dorsal root ganglion neurons. Eur J Anaesthesiol. 2007;24(11):934–41.
13. Chen BS, Peng H, Wu SN. Dexmedetomidine, an alpha2-adrenergic agonist, inhibits neuronal delayed-rectifier potassium current and sodium current. Br J Anaesth. 2009;103(2):244–54.
14. Dib-Hajj SD, Cummins TR, Black JA, Waxman SG. Sodium channels in normal and pathological pain. Annu Rev Neurosci. 2010;33:325–47.
15. Fan N, Donnelly DF, LaMotte RH. Chronic compression of mouse dorsal root ganglion alters voltage-gated sodium and potassium currents in medium-sized dorsal root ganglion neurons. J Neurophysiol. 2011;106(6):3067–72.
16. Cummins TR, Sheets PL, Waxman SG. The roles of sodium channels in nociception: Implications for mechanisms of pain. Pain. 2007;131(3):243–57.
17. Dib-Hajj SD, Binshtok AM, Cummins TR, Jarvis MF, Samad T, Zimmermann K. Voltage-gated sodium channels in pain states: role in pathophysiology and targets for treatment. Brain Res Rev. 2009;60(1):65–83.
18. Renganathan M, Cummins TR, Waxman SG. Contribution of Na(v)1.8 sodium channels to action potential electrogenesis in DRG neurons. J Neurophysiol. 2001;86(2):629–40.
19. Akopian AN, Souslova V, England S, Okuse K, Ogata N, Ure J, et al. The tetrodotoxin-resistant sodium channel SNS has a specialized function in pain pathways. Nat Neurosci. 1999;2(6):541–8.
20. Lai J, Gold MS, Kim CS, Bian D, Ossipov MH, Hunter JC, et al. Inhibition of neuropathic pain by decreased expression of the tetrodotoxin-resistant sodium channel, NaV1.8. Pain. 2002;95(1–2):143–52.
21. Ekberg J, Jayamanne A, Vaughan CW, Aslan S, Thomas L, Mould J, et al. muO-conotoxin MrVIB selectively blocks Nav1.8 sensory neuron specific sodium channels and chronic pain behavior without motor deficits. Proc Natl Acad Sci U S A. 2006;103(45):17030–5.
22. Cang CL, Zhang H, Zhang YQ, Zhao ZQ. PKCepsilon-dependent potentiation of TTX-resistant Nav1.8 current by neurokinin-1 receptor activation in rat dorsal root ganglion neurons. Mol Pain. 2009;5:33.
23. Shirasaka T, Kannan H, Takasaki M. Activation of a G protein-couple inwardly rectifying K^+ current and suppression of Ih contribute to dexmedetomidine-induced inhibition of rat hypothalamic paraventricular nucleus neurons. Anesthesiology. 2007;107(4):605–15.

24. Ramos BP, Stark D, Verduzco L, van Dyck CH, Arnsten AF. Alpha2A-adrenoceptor stimulation improves prefrontal cortical regulation of behavior through inhibition of cAMP signaling in aging animals. Learn Mem. 2006;13(6):770–6.
25. Akopian AN, Sivilotti L, Wood JN. A tetrodotoxin-resistant voltage-gated sodium channel expressed by sensory neurons. Nature. 1996;379(6562):257–62.
26. Su YY, Ye M, Li L, Liu C, Pan J, Liu WW, et al. KIF5B promotes the forward transport and axonal function of the voltage-gated sodium channel Nav1.8. J Neurosci. 2013;33(45):17884–96.
27. Lampert A, O'Reilly AO, Reeh P, Leffler A. Sodium channelopathies and pain. Pflugers Arch. 2010;460(2):249–63.
28. Fan N, Sikand P, Donnelly DF, Ma C, Lamotte RH. Increased Na + and K+ currents in small mouse dorsal root ganglion neurons after ganglion compression. J Neurophysiol. 2011;106(1):211–8.
29. Wang JG, Strong JA, Xie W, Zhang JM. Local inflammation in rat dorsal root ganglion alters excitability and ion currents in small-diameter sensory neurons. Anesthesiology. 2007;107(2):322–32.
30. Tanaka M, Cummins TR, Ishikawa K, Dib-Hajj SD, Black JA, Waxman SG. SNS Na + channel expression increases in dorsal root ganglion neurons in thecarrageenan inflammatory pain model. Neuroreport. 1998;9(6):967–72.
31. Gould 3rd HJ, England JD, Liu ZP, Levinson SR. Rapid sodium channel augmentation in response to inflammation induced by complete Freund's adjuvant. Brain Res. 1998;802(1–2):69–74.
32. Laird JM, Souslova V, Wood JN, Cervero F. Deficits in visceral pain and referred hyperalgesia in Nav1.8 (SNS/PN3)-null mice. J Neurosci. 2002;22(19):8352–6.
33. Joshi SK, Mikusa JP, Hernandez G, Baker S, Shieh CC, Neelands T, et al. Involvement of the TTX-resistant sodium channel Nav 1.8 in inflammatory and neuropathic, but not post-operative, pain states. Pain. 2006;123(1–2):75–82.
34. Black JA, Liu S, Tanaka M, Cummins TR, Waxman SG. Changes in the expression of tetrodotoxin-sensitive sodium channels within dorsal root ganglia neurons in inflammatory pain. Pain. 2004;108(3):237–47.
35. He XH, Zang Y, Chen X, Pang RP, Xu JT, Zhou X, et al. TNF-α contributes to up-regulation of Nav1.3 and Nav1.8 in DRG neurons following motor fiber injury. Pain. 2010;151(2):266–79.
36. Jarvis MF, Honore P, Shieh CC, Chapman M, Joshi S, Zhang XF, et al. A-803467, a potent and selective Nav1.8 sodium channel blocker, attenuates neuropathic and inflammatory pain in the rat. Proc Natl Acad Sci U S A. 2007;104(20):8520–5.
37. Belkouch M, Dansereau MA, Réaux-Le Goazigo A, Van Steenwinckel J, Beaudet N, Chraibi A, et al. The chemokine CCL2 increases Nav1.8 sodium channel activity in primary sensory neurons through a Gβγ-dependent mechanism. J Neurosci. 2011;31(50):18381–90.
38. Millan MJ, Newman-Tancredi A, Audinot V, Cussac D, Lejeune F, Nicolas JP, et al. Agonist and antagonist actions of yohimbine as compared to fluparoxan at alpha(2)-adrenergic receptors (AR)s, serotonin (5-HT)(1A), 5-HT(1B), 5-HT(1D) and dopamine D(2) and D(3) receptors. Significance for the modulation of frontocortical monoaminergic transmission and depressive states". Synapse. 2000;35(2):79–95.
39. Nicholas AP, Pieribone V, Hökfelt T. Distributions of mRNAs for alpha-2 adrenergic receptor subtypes in rat brain: an in situ hybridization study. J Comp Neurol. 1993;328(4):575–94.
40. Cho HJ, Kim DS, Lee NH, Kim JK, Lee KM, Han KS, et al. Changes in the alpha 2-adrenergic receptor subtypes gene expression in rat dorsal root ganglion in an experimental model of neuropathic pain. Neuroreport. 1997;8(14):3119–22.
41. Chung K, Kim HJ, Na HS, Park MJ, Chung JM. Abnormalities of sympathetic innervation in the area of an injured peripheral nerve in a rat model of neuropathic pain. Neurosci Lett. 1993;162(1–2):85–8.
42. Cheng HJ, Ma KT, Li L, Zhao L, Wang Y, Si JQ. Differential expression of alpha-adrenoceptor subtypes in rat dorsal root ganglion after chronic constriction injury. J Huazhong Univ Sci Technolog Med Sci. 2014;34(3):322–9.
43. Chen SR, Pan HM, Richardson TE, Pan HL. Potentiation of spinal alpha(2)-adrenoceptor analgesia in rats deficient in TRPV1-expressing afferent neurons. Neuropharmacology. 2007;52(8):1624–30.
44. Bavencoffe A, Gkika D, Kondratskyi A, Beck B, Borowiec AS, Bidaux G, et al. The transient receptor potential channel TRPM8 is inhibited via the alpha 2A adrenoreceptor signaling pathway. J Biol Chem. 2010;285(13):9410–9.
45. Matsumoto S, Yoshida S, Ikeda M, Tanimoto T, Saiki C, Takeda M, et al. Effect of 8-bromo-cAMP on the tetrodotoxin-resistant sodium (Nav 1.8) current in small-diameter nodose ganglion neurons. Neuropharmacology. 2007;52(3):904–24.